Available online at www.sciencedirect.com
SCIENCE DIRECT®
Journal of Molecular Catalysis A: Chemical 219 (2004) 131–141
JOURNAL OF MOLECULAR CATALYSIS A: CHEMICAL
www.elsevier.com/locate/molcata

Direct observation of thermally activated NO adsorbate species on Au–TiO_2: DRIFTS studies

M.A. Debeila*, N.J. Coville, M.S. Scurrell*, G.R. Hearne

Molecular Sciences Institute, School of Chemistry, Private Bag X3, University of the Witwatersrand, Johannesburg 2050, South Africa

Received 16 March 2004; accepted 29 April 2004

Available online 9 June 2004

Abstract

Adsorption of nitric oxide on Au–TiO_2 catalyst prepared by impregnation to incipient wetness was carried out using DRIFTS as a monitoring technique. Highly dispersed Au particles covering the TiO_2 support and blocking most sites (on TiO_2) for NO adsorption is indicated. The early spectra are dominated by M–ONO^- (monodentate as well as bridging nitrito surface species) which disappear following an increase in NO pressure, presumably due to conversion to nitrate species which dominate the spectra after extended exposure to NO. Nitrate species decompose at high temperature to form NO_2^- species that coordinated to the surface as N-donor nitro complexes. Two characteristic bands due to ν(N–O) bond vibrations (1690–1696 and 1654 cm^{-1}) of adsorbed NO at different sites were obtained on contact of the sample with NO. These bands are significantly red shifted relative to gas phase NO. The sites to which these NO adsorbates are bonded are populated first and represent the most stable sites for NO adsorbates on catalyst studied here at room temperature. The lower wavenumber band (1654 cm^{-1}) desorbed and/or dissociated during NO adsorption and is tentatively assigned to NO adsorbed on interfacial sites involving both Au and TiO_2 support (Au–oxide interface) and/or Au sites in the vicinity of oxygen vacancy. The NO adsorbed state with absorption band at 1696–1690 cm^{-1}, assigned to bridging sites, change from one adsorbed state to another at elevated temperatures, i.e. it decreased in intensity and red shifted to lower wavenumbers with concomitant development and growth of two bands at 1748–1754 and 1722–1730 cm^{-1} during progressive increase in the temperature of the system. Another pair of bands (2182–2178 and 2162 cm^{-1}) developed at temperatures >100 °C. These are due to thermally activated NO adsorbate states and are thermally stable. Reported data suggests that these NO adsorbates are bound on low valent and/or unstable high intrinsic energy edge Au sites. It is suggested that these thermally stable surface 'Au=NO' complexes are formed by altering the local atomic geometry to achieve higher stability, and once formed, they are irreversible.

Keywords: Au–TiO_2; NO; Adsorption; Thermally stable; DRIFTS

1. Introduction

With the increase in global air pollution, efforts are continually being made to obtain more effective catalytic materials for use in various pollutant abatement processes. Various metals supported on a range of supports have been investigated for this process. Following a breakthrough in the use of gold as a heterogeneous catalyst [1], a large number of reports demonstrating the high activity of supported gold catalysts emerged [2]. The extensively studied reaction is low temperature carbon monoxide oxidation [3–6]. One application of supported gold catalysts which is currently being investigated is the catalytic reduction of NO_x to $N_2 + O_2$ with hydrocarbons [7–12] or CO [13–16] as reductants. Reduction of NO by CO in the absence of O_2 was reported to occur at temperatures below 100 °C, yielding N_2 as the major product [16]. Gold supported on TiO_2, ZnO, MgO and Al_2O_3 also showed high activity for the reduction of NO with propylene at high temperatures (500 °C) [12]. Addition of Mn_2O_3 to Au–Al_2O_3 was shown to enhance NO_2 formation and improve the conversion of NO to N_2 [10]. This composite catalyst offers one of the best performances for NO conversion since it can maintain high conversion over a wide temperature range [10]. Cobalt promoted gold catalysts formulated for use in gasoline and diesel applications showed a conversion window at temperatures between 220 and 350 °C with maximum conversion at 290 °C [17].

* Corresponding authors. Tel.: +27-11-717-6761; fax: +27-11-717-6749.
E-mail addresses: abel2000za@yahoo.com (M.A. Debeila), scurrell@aurum.wits.ac.za (M.S. Scurrell).

1381-1169/$ – see front matter © 2004 Elsevier B.V. All rights reserved.
doi:10.1016/j.molcata.2004.04.033

Despite these efforts, the surface chemistry associated with the adsorption and reaction of nitric oxide on supported Au catalysts is not well understood. Studies using infrared spectroscopy have shown that a variety of adsorbed species can exist on gold supported on zeolites [18,19] and TiO_2 [20–22]. Direct decomposition of NO on Au(I)/NaY catalysts to N_2 and O_2 in the temperature range 300–673 K were reported [18]. However, the authors did not obtain steady-state activities. The delayed evolution of oxygen observed in their experiments led them to suggest the formation of gold oxide which is decomposed at higher temperature [18]. Recently, Solymosi et al. [21,22] studied the adsorption of NO on 6 nm Au particles supported on TiO_2. The authors observed bands at 1747 and 1583 cm^{-1} [21] and 1767 and 1747 cm^{-1} [22] attributed to the vibration of NO bonded to an Au site. These bands are significantly red shifted relative to gas phase NO (1876 cm^{-1}). Though strongly bound oxygen on the catalysts surface is presumed to prevent further decomposition of NO [23], the thermally activated NO adsorbate species observed in this study might shed some light on other surface species that might have similar effects. In earlier work we have also described a mechanism of adsorption of NO on TiO_2 [24].

In this article, we report further on the surface species produced upon adsorption of NO on Au–TiO_2. The species are identified and discussed in terms of structural models derived for gold surfaces. Comparison is also made with models derived for other metal catalysts. Thermal stability is assessed by thermal desorption experiments using in situ DRIFTS. We report for the first time the formation of NO adsorbate species on Au–TiO_2 formed via a thermal activation process. These NO species have a high thermal stability and their formation may have important implications for the catalytic conversion of NO.

2. Experimental

DRIFTS spectra were recorded on a Nicolet Impact 420 IR spectrometer, equipped with a DTGS KBr detector at a spectral resolution of 4 cm^{-1} as described elsewhere [20,24]. The fine powdered samples were loaded into a sample cell (Harrick Scientific) equipped with a ZnS window, which allowed treatment of samples under various controlled atmospheres. Gases were supplied by Afrox Ltd. and were used as supplied.

The 5 wt.% Au–TiO_2 samples were prepared by impregnation to incipient wetness of titania (Degussa P-25, comprising ~80% anatase and 20% rutile phase). The BET surface area of the TiO_2 ~49 m^2/g, with total pore volume of 0.170 cm^3/g and average pore diameter of 14.0 nm and particles were in the size range 1150–850 μm. Deionized water was used to dissolve the $HAuCl_4$, and after impregnation the sample was dried at 150 °C for 16 h. the catalyst was calcined at 400 °C in 5% O_2/He mixture (flow rate of 30 ml/min) and gave Au–TiO_2 with BET surface area of ~45 m^2/g, total pore volume of ~0.413 cm^3/g and average pore diameter of 36.9 nm. The sample was loaded into the DRIFTS cell and flushed with helium (flow rate: 30 ml/min). The temperature of the system was raised at a rate of 10°/min to 300 °C and held at this temperature for 2 h and then cooled to room temperature. Since this temperature is below that used for calcination, and is also the highest temperature used during the thermal desorption, no significant additional sintering is expected to occur during the IR experiments. The background spectrum of the pre-treated catalysts was measured at room temperature prior to NO (0.3% NO in He) adsorption measurements. Typically 1024 scans were accumulated per run. The experiment was conducted in a flow mode, however, in the first two spectra recorded (Fig. 1a and b), in order to suppress as much as possible the sequential reaction of adsorbed species with NO, NO was introduced in small amounts to pre-treated Au–TiO_2 at ~0.3 bar. Before increasing the NO pressure, a steady-state flow of NO was maintained (Fig. 1c–f).

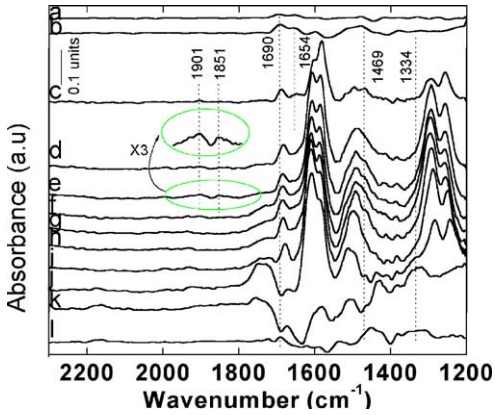

Fig. 1. IR spectra of NO adsorbed on Au–TiO_2 calcined at 400 °C. Gas (0.3% NO in He) was introduced at: (a) 0.3 bar, 20 min; (b) 0.3 bar, 20 min; (c) 0.3 bar, flow mode; (d) 1 bar, flow mode; (e) 2 bar, flow mode; (f) 2 bar, flow mode. Purging with He gas (UHP) was then carried out at: (g) 25 °C; (h) 50 °C; (i) 100 °C; (j) 200 °C; (k) 300 °C; (l) cooled to 25 °C.

3. Results

DRIFTS spectra were recorded for this catalyst in contact with NO as a function of time (Fig. 1a–c), pressure Fig. 1d–e) and also for an extended period of time (Fig. 1f). Interaction of the catalyst with NO resulted in a spectrum with bands at 1696, 1654, 1595 (weak), 1480, 1325 and 1277 cm^{-1}. The weak band observed at 1595 cm^{-1} (Fig. 1a–c), was later replaced, by two bands at 1600 and 1584 cm^{-1} (with maximum at 1600 cm^{-1} appearing as a shoulder on the 1584 cm^{-1} band). These bands increased in intensity and blue shifted to 1609 and 1587 cm^{-1} with increased NO pressure (Fig. 1e) and extended exposure to NO (Fig. 1f). It is also noted that the two bands exchanged intensity with the 1609 cm^{-1}, band becoming stronger than

the 1587 cm^{-1} band. At the same time, two bands developed in the lower wavenumber region at 1296 (broad) and 1257 cm^{-1} with the latter being slightly more intense. There is also the corresponding exchange in intensity in the lower wavenumber region (Fig. 1d). The band observed at 1480 cm^{-1} was sharp and increased in intensity in the first stages of NO adsorption (Fig. 1a and b) before it decreased in intensity and was replaced by a broad and low intensity band with maxima at 1467 and 1497 cm^{-1} (Fig. 1c). Further increase in the NO pressure and extended exposure of the sample to NO resulted in an increase in the intensity of this band with further broadening and the two maxima seem to overlap (Fig. 1d–f). However, a shoulder is still visible on the lower wavenumber side of this band. This band also blue shifted to 1487 cm^{-1} under these conditions. The three bands (1609, 1587 and 1487 cm^{-1}) grew in parallel with two bands at 1295 cm^{-1} (strong) and 1257 cm^{-1} (medium). Another weak band is observed at 1518 cm^{-1} (Fig. 1a) (drastically decreased in intensity with increased pressure to 2 bar, Fig. 1d) i.e. this eventually disappeared and/or overlapped with the broad band centred at 1487 cm^{-1} following prolonged exposure to NO. Certain features of the spectra in Fig. 1 are very similar to those obtained following the adsorption of NO on TiO_2 [24]. This similarity suggests that the addition of Au on TiO_2 did not significantly alter the adsorption sites for these species. The bands at 1609, 1587 and 1487 cm^{-1} were previously assigned to three differently coordinated nitrate species [24]. Other spectral features are largely attributed to NO entities associated with Au sites (see below). The assignment of the bands observed in this study is made in Table 1.

Desorption of adsorbed species from Au–TiO_2 was monitored as a function of temperature, Fig. 1f–k. The nitrate species were stable to flushing with He at room temperature (Fig. 1f–g). At 200 °C, spectral changes are noted (Fig. 1j). The band associated with monodentate nitrate moved to higher wave numbers with a decrease in intensity (1487 cm^{-1} after 10 h, 1498 cm^{-1} at 100 °C and 1513 cm^{-1} at 200 °C, Fig. 1f–j). There is also a corresponding decrease in intensity and shift in position of the lower wavenumber component at 1292 cm^{-1} which red shifted to 1282 cm^{-1}. However, bands for bridging and bidentate nitrate species were only slightly affected. This behaviour was reported and discussed previously for NO on TiO_2 [24]. On raising the temperature to 300 °C, bands associated with nitrates were virtually all removed with only remnant bands being visible at 1587, 1511 cm^{-1}. New bands appeared at 1428 together with a broad band centred at 1327 cm^{-1} (Fig. 1l). On cooling the system to room temperature, bands were seen at 1535 cm^{-1} (medium), 1452–1428 cm^{-1} (broad) and 1350–1311 cm^{-1}.

The bands at 1452–1428 cm^{-1} could be assigned to $\nu_{asym}(NO_2)$ of M–NO_2 species. The corresponding $\nu_{sym}(NO_2)$ is seen at 1350–1311 cm^{-1} [25]. The band at 1518 cm^{-1} that disappeared with increased pressure to 2 bar, is within the region expected for μ(N,O) bridging nitrito

Table 1
Peak positions (cm^{-1}) and assignment of the surface complexes detected on Au–TiO_2

Assigned surface species	NO addition, at 0.3 bar	NO, flow mode at 0.3 bar	NO, flow mode at 1 bar	NO, flow mode at 2 bar	He purge, at 25 and 50 °C	He purge at 100 °C	He purge at 200 °C	He purge at 300 °C	Cooled to 25 °C
AuNO	1654, 1696	1654 (vw), 1690	nd, 1688	nd, 1684, 1733 (vw)	nd, 1684, 1733 (vw)	nd, 1678, 1748, 1722	nd, 1671, 1748, 1722, 2182–2178, 2162	nd, 1671, 1754, 1730, 2182–2178, 2162	nd, 1690, 1748, 1722, 2182–2178, 2162
NO_2^- (bridging nitrito)	1518	1518	1501 (vw)	nd	nd	nd	nd	1511	1535
NO_2^- (unidentate nitrito)	1480	1480	1467 (w)	nd	nd	nd	nd	nd	nd
NO_2^- (nitro)	1416, 1325	1436 (sh), 1331	1654 cm^{-1} (vw)	nd	nd	nd	nd	1428, 1327–1311	1452–1428, 1327–1311
NO_3^- (monodentate)	nd	nd	1497, 1301	1487, 1292	1491, 1289	1497, 1289	1509, 1286	1509, –	nd
NO_3^- (bidentate)	nd	nd	1585, 1292	1587, 1292	1587, 1289	1587, 1289	1587, 1286	1584, –	1587 (vw)
NO_3^- (bridging)	nd	nd	1602, 1257	1609, 1255	1609, 55	1609, 1255	1609, 1247	1609, 1242	nd

nd: not detected, vw: very weak, w: weak, sh: shoulder.

surface species [25,26]. These species seems to reappear at high temperature. In the spectrum recorded at 300 °C a band was detected at 1511 and at 1535 cm^{-1} on cooling to room temperature (Table 1). The observation of bands associated with M–NO_2 complexes (dominant after cooling the system to room temperature, Fig. 1l) on a surface previously dominated by nitrate species, suggests decomposition of nitrates (NO_3^-) to nitrites (NO_2^-) [27,28].

For Au–TiO_2 catalysts there are virtually no bands associated with nitrosyl complexes in the region 2000–1700 cm^{-1} (Fig. 1, curve f). Very weak bands at 1905 and 1851 cm^{-1} (shown in expanded scale in the inset in Fig. 1), appeared with increased pressure of NO to 2 bar (Fig. 1d), but eventually disappeared on extended exposure to NO. These bands have previously been detected following adsorption of NO on TiO_2 and are characteristic of Ti^{4+}(NO) complexes [24]. The low intensity of these bands for Au–TiO_2 compared to TiO_2 [24] suggests that most sites might be blocked [29] by Au. Two bands with maxima at 1696 and 1654 cm^{-1} were detected after first contact of NO with the sample. These bands have not been previously observed on TiO_2 under identical experimental conditions [24] and need further discussion (see Fig. 2).

Fig. 2 summarizes the behaviour of these two bands under our experimental conditions. The band at 1696 cm^{-1} grew with time (Fig. 1a–c), and reached saturation on increasing the pressure of NO to 2 bar (Fig. 1d) and thereafter slightly decreased in intensity following extended exposure to NO (Fig. 1f). The lower wavenumber band (1654 cm^{-1}) eventually disappeared on increasing the pressure of NO to 2 bar (Fig. 1d). The band at 1696 cm^{-1} red shifted with time (1690 cm^{-1}) (Fig. 2a and b) and on increasing the pressure

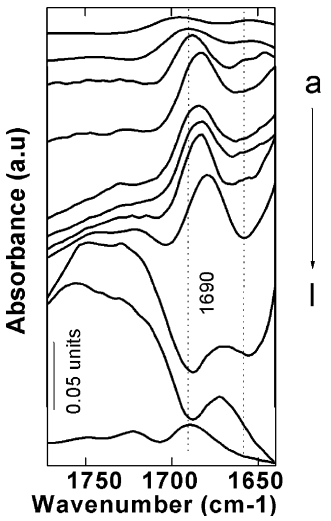

Fig. 2. IR spectra of NO adsorbed on Au–TiO_2, showing only the region, 1800–1640 cm^{-1}. Gas (0.3% NO in He) was introduced at: (a) 0.3 bar, 20 min; (b) 0.3 bar, 20 min; (c) 0.3 bar, flow mode; (d) 1 bar, flow mode; (e) 2 bar, flow mode; (f) 2 bar, flow mode. Purging with He gas (UHP) was then carried out at: (g) 25 °C; (h) 50 °C; (i) 100 °C; (j) 200 °C; (k) 300 °C; (l) cooled to 25 °C.

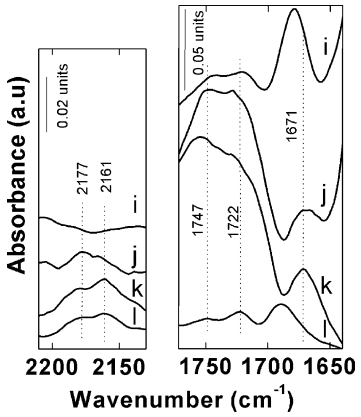

Fig. 3. IR spectra of NO adsorbed on Au–TiO_2 showing the regions, 1800–1640 and 2210–2130 cm^{-1} during purging with He gas, at: (i) 100 °C; (j) 200 °C; (k) 300 °C; (l) 25 °C (cooled from 300 °C).

of the system to 2 bar (1684 cm^{-1}) (Fig. 1d). After that it seemed to remained practically constant in position with further increase in pressure and prolonged exposure to NO (Fig. 2e and f), and following flushing with He at room temperature and at 50 °C (Fig. 1g and h). Fig. 2 shows that after 10 h of exposure, there is a broad and ill-defined feature in the region centred at ~1731 cm^{-1} only after extended exposure to NO. Following flushing with He at room temperature and at 50 °C (Fig. 1g and h), this weak feature seems to remain essentially unchanged. On raising the temperature to 100 °C, the band further red shifted to 1678 cm^{-1} (Fig. 2i). At this stage the weak and broad feature increased in intensity and poorly resolved maxima can now be distinguished at 1748 and 1722 cm^{-1}. Further increase in temperature to 200 °C led to an increase in the intensity of bands at 1748 and 1722 cm^{-1} (Fig. 1i and j). At this temperature (200 °C), there is a development of a further two poorly resolved bands with distinguishable maxima at 2182–2178 and 2162 cm^{-1}. These bands are shown in expanded scale in Fig. 3. At the same time, the band observed at 1678 cm^{-1} further decreased in intensity and red shifted to 1671 cm^{-1}. Increasing the temperature to 300 °C resulted in a slight decrease in intensity of the bands at 1748 and 1722 cm^{-1} and a slight blue shift to 1754 and 1730 cm^{-1}, respectively. At the same time (i.e. at 300 °C) the two bands at 2178–2182 and 2162 cm^{-1} increased in intensity (Fig. 2k). However, the band at 1671 cm^{-1} seemed to remain practically constant. Note that the negative absorption peak at ~1634 cm^{-1} is most likely due to δ(HOH) [30] and makes proper assessment of the band at 1671 cm^{-1} difficult. Note that the bands due to thermally activated NO adsorptions in the two regions (i.e. 1754–1748 and 1730–1722 cm^{-1} and at 2178–2182 and 2162 cm^{-1}) occur in *pairs*. On cooling the system to room temperature (still under flowing He gas): (i) the band at 1671 cm^{-1} disappeared (Fig. 2l); (ii) the broad band observed at 1754–1730 cm^{-1} and 2178–2182 and 2162 cm^{-1} decreased in intensity with remnant bands at 1748 and 1722 cm^{-1}, and at 2182–2178 and 2162 cm^{-1};

(iii) the band at 1690 cm^{-1} re-emerged (compare curves b and l of Fig. 2). Since these bands were not detected for TiO_2 under identical experimental conditions [24], we believe they are associated with NO adsorbates on gold containing sites. It is important to note that the nature of the adsorbed species detected on the surface depends on how the probe gas was first introduced to the sample. For example, the bands at 1696 and 1654 cm^{-1} were detected only when NO was introduced in small amounts at the beginning and spectrum recorded following each addition (Fig. 1a and b). When the first contact of NO with the sample is made through continuous flow, extensive sequential reactions of NO with adsorbed species takes place and the spectrum is immediately dominated by nitrate bands. Under these conditions, a low intensity band at 1680 cm^{-1} is detected, while the band at 1654 cm^{-1} is not detected (spectrum not shown).

The bands in the region 1700–1500 cm^{-1} may also characterize higher nitrogen oxides, e.g. N_2O_4 and N_2O_3. To explore this possibility, and to aid in the assignment, adsorption of NO_2 under identical conditions was carried out. The results, which will be published elsewhere [31] show initial spectra with bands at 1673 and 1656 cm^{-1} which disappeared with increasing pressure of NO_2. During the desorption at elevated temperatures, no bands in the region 1700–1600 cm^{-1} were detected.

4. Discussion

4.1. NO_2^- and NO_3^- entities

The formation of NO_2^- and NO_3^- complexes on TiO_2 was outlined previously [24] and only the differences will be highlighted in this paper.

After 90 min of exposure of catalyst to NO, bands associated with nitrate species were already dominant and after 2 h exposure, the spectrum recorded was already similar to that obtained after 10 h exposure to NO on TiO_2 [24]. It is suggested that less oxygen was available for the formation of NO_2^- and/or NO_3^- with (NO + TiO_2) than for (NO + Au–TiO_2). The source of the additional oxygen cannot be established from the present data alone. However, an investigation of the low temperature catalytic decomposition of NO on Au(I)/NaY-zeolites carried out by Salama et al. [18] provides information for understanding the interaction between Au(I)/NaY and NO. The important finding is that decomposition of NO was taking place, even at room temperature, resulting in the formation of gold oxide, which was decomposed at 423 K with the resultant evolution of O_2. Oxidized Au–TiO_2 provides an ideal surface to dissociate NO (see above) and the oxygen atoms (from dissociated NO) that remain on the surface under the conditions used in this study [18], might supply the extra oxygen for the reaction [24].

The disappearance of nitrate bands and the simultaneous appearance of bands characteristic of nitro complexes suggest that the decomposition of NO_3^- results in the formation of NO_2^- species [27,28]. This contrasts with the situation for TiO_2 [24] in which the bonding mode of NO_2^- to the surface, following decomposition of NO_3^-, was dominated by monodentate oxygen nitrito surface complexes (M–ONO^-) [24]. Hence the addition of Au onto TiO_2 led to a change in the bonding configuration of NO_2^- to the surface. Coordination of nitrite to a metal can involve several configurations [25,32], depending on several factors such as electronic, steric and kinetic factors [32] although the relative importance and the manner in which these determine the coordination geometry of NO_2^- to the metal is not well understood. According to the classification by Huheey et al. [33], Ti^{4+} is a hard acid and Au^+ is a soft acid. It is therefore expected that metallic Au atom is softer than the Au^+ ion. When NO_2^- is bonded to the metal through oxygen, it acts as a π donor and a hard base, whereas when bonded through the nitrogen atom, it functions as a π acceptor and soft base [32]. Therefore, it is not surprising that M–NO_2 are dominant species for Au–TiO_2 whereas M–ONO^- dominate on TiO_2 surface [24]. The presence of a high frequency stretching mode (ν(N=O)) that is associated with coordination of NO_2^- through both a nitrogen and an oxygen atom [25,32] seen in this study (band at 1501–1518 cm^{-1}) suggests that this bonding geometry is likely to be present.

4.2. Au monomeric complexes

The most important molecular orbitals associated with the NO molecule in determining its reactivity, are a non-bonding 5σ molecular orbital on the nitrogen atom which acts as a donor level and the $2\pi^*$ antibonding molecular orbital which acts as both a donor and an acceptor level. This acceptor/donor character of NO is responsible for the multiple modes of coordination of NO to a metal (M) in metal nitrosyl compounds [34].

The vibrational frequency of N–O bond for nitrosyl complexes on metals and metal oxides falls between 2200 and 1000 cm^{-1} depending on the type of bonding to the surface [35–39]. The positions of the bands reported in this paper are significantly lower than ν(N–O) of Au–NO complexes reported previously [20,40]. Several experiments examining NO adsorption on Pt and Pd surfaces have been carried out and Table 2 [41–46] demonstrates the geometric versatility of NO as an adsorbate on these surfaces and Fig. 4 shows possible configurations of adsorbed NO at different sites. The observed geometries include bridging, linear atop and bent atop arrangement [42]. Binding energies for NO vary dramatically with coverage, and shifts in binding energies are due to the changes in adsorption geometry [47]. At low coverage, NO is reported to exist in bridging sites but at higher coverage, linear atop NO can be observed, e.g. on Pt(1 1 1) [48].

Inspection of Fig. 2 shows that two bands (1696 and 1654 cm^{-1}) are the dominant ones in the initial spectra and are almost equally intense on exposure of the sample to NO,

Table 2
Experimentally determined vibrational frequencies of MNO states (M = Pd and Pt)

Catalyst	Frequency (cm^{-1})	Structure and/or site	Ref.
Pt(1 0 0)	1645	Bent atop	[41]
Pt(1 0 0)	1757	Linear atop	[41]
Pt(1 0 0)	1660	Bent atop	[42]
Pt(1 0 0)	1790	Linear atop	[42]
Rh/Y-zeolites	1700	Bridge bonded	[43]
Pd(1 1 1)	1736	Bent	[44]
Pd(1 0 0)	1632–1599	Three-fold sites	[45]
Pd(1 1 1)	1580–1572	Four-fold sites	[45]
Pd/Al_2O_3	1690	Bridge bonded	[46]
	1680	Atop and step bound	[46]

suggesting that the two sites might be populated with equal probability, and thus the energetics for their population might be similar. These sites are populated first, and thus represent the most stable sites for NO adsorption on this catalyst at room temperature. The shift of the band at 1696 cm^{-1} to lower wavenumbers, suggests that the dipole–dipole coupling effect between NO adsorbate species on these sites is negligible [46].

It has been established that linearly bound CO molecules on supported gold catalysts exhibits unusual coverage-dependent shifts to lower wavenumbers as the coverage increases [49]. This is the exact opposite to that expected from dipole–dipole coupling effects which causes the absorption band to shift to higher wavenumbers as the coverage increases. Mixed isotope experiments have shown that the behaviour is due to the existence of a large and negative chemical shift [50–52]. Similar coverage-dependent shifts for NO adsorbates on gold surfaces have not been reported before. Since the band at 1696 cm^{-1} continued to shift to lower wavenumbers even during desorption with He gas in which dipole coupling effects for NO are expected to be reduced, a coverage-dependent shift for the band at 1696 cm^{-1} is ruled out. The observations are: (i) the band at 1696 cm^{-1} shifted to lower wavenumbers with decrease in intensity (Fig. 2a–k); (ii) there is a development and growth of two bands at 1748–1754 and 1722–1730 cm^{-1} and further at 2182–2178 and 2162 cm^{-1} (at temperatures > 100 °C); (iii) on cooling the system to room temperature, the band at 1690 cm^{-1} re-emerged at its original position concomitant with a decrease in intensity of the bands at 1748–1754 and 1722–1730 cm^{-1} and at 2182–2178 and 2162 cm^{-1} (compare Fig. 2b and l). These features suggest that the NO adsorbate state responsible for the absorption band at 1690–1696 cm^{-1} is a likely precursor state for the activated NO adsorbate species responsible for the absorption bands at 1748–1754 and 1722–1730 cm^{-1} and/or at 2182–2178 and 2162 cm^{-1}. Further it is noted that: (i) no activated NO adsorbate states (with absorption bands in the region 1748–1754 and 1722–1730 cm^{-1} and at 2182–2178 and 2162 cm^{-1}) were detected, in the absence of the precursor NO adsorbate (band at around 1696–1690 cm^{-1} region), on the same catalyst under identical conditions following adsorption of NO_2 [31], and/or after adsorption of NO on TiO_2 [24]; (ii) the activated NO adsorbate states developed during flushing with He, long after NO feed gas to the system was terminated (Fig. 2). Point (i) above also suggests that the contributions from the decomposition of NO_2^- and/or NO_3^- species to the activated NO adsorbate states (bands at 1748–1754, 1722–1730 cm^{-1} and at 2182–2178 and 2162 cm^{-1}) are negligible under our experimental conditions. It is also evident from Fig. 2 that the activated NO adsorbate states only require a precursor state with a band at 1690 cm^{-1}. This stems from the fact that the activated NO adsorbate states developed despite the absence of species with absorption bands at 1656–1654 cm^{-1} (Fig. 2).

Fig. 2 shows that the two NO activated adsorbate species with absorption bands at 1748 and 1722 cm^{-1} are already intense at 200 °C (appeared to have reached saturation at this temperature) and an ill-defined feature is visible in the region 1748–1722 cm^{-1} at room temperature only after extended exposure of the catalyst to NO (Fig. 2f). This weak feature increased in intensity with progressive increases in temperature (Fig. 2f–k). It is suggested that a very small fraction of these sites (states with bands at 1748–1754 and 1722–1730 cm^{-1}) are populated at room temperature, and the rest are significantly populated at elevated temperatures. The sites containing NO adsorbates with absorption bands at 2182–2178 and 2162 cm^{-1} are populated at even higher temperatures (i.e. temperatures > 100 °C) (Fig. 3).

The fact that the precursor state (with band at 1690 cm^{-1}) and the product states (with bands at 1748–1754 and 1722–1730 cm^{-1} and at 2182–2178 and 2162 cm^{-1}) could be detected on the surface at the same time (Fig. 2i and j) suggests that not all NO adsorbate molecules (band at 1690 cm^{-1}) are converted to the new states (1748–1754 and 1722–1730 cm^{-1} and at 2182–2178 and 2162 cm^{-1}) at once and, further, the precursor and the product species can co-exist on the surface. Co-existence of these surface states (the precursor and the products) indicates the presence of a variety of different local environments on the surface.

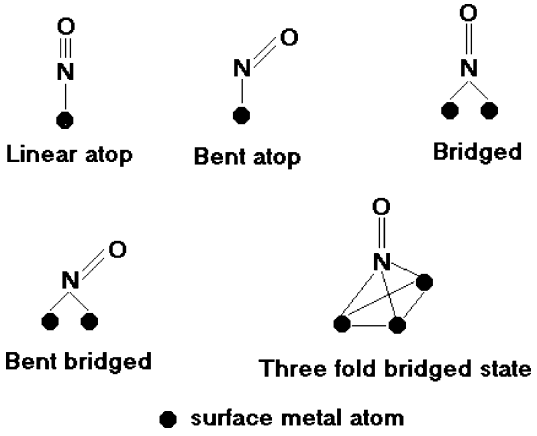

Fig. 4. Possible arrangements of NO in MNO complexes.

The observation of the re-emergence of the band at 1690 cm^{-1} on cooling the system to room temperature (from 300 °C) with concomitant decrease in intensity of the bands at 1748–1754 and 1722–1730 cm^{-1} and at 2182–2178 and 2162 cm^{-1} (Fig. 2l) suggests that the transition between these surface states is incomplete even at 300 °C. This suggests that the transitions between the NO adsorbate states are partially reversible at temperatures below 300 °C. This can be explained by considering different local environments on the surface (see above) for which different (a distribution of) activation energies for the population of the sites (and also for a complete transition) exist. The remnant bands (at 1748 and 1722 cm^{-1} and at 2182–2178 and 2162 cm^{-1}) remaining after cooling the system to room temperature can be explained by assuming that the NO adsorbates associated with these bands have assumed relatively stable surface configurations (as a results of thermal processing), i.e. more stable surface 'AuNO' complexes. This suggests that once the thermally stable surface complexes are formed they cannot be reversed to the precursor state on termination of heat.

The existence of different local environments on the surface is further evidenced by the fact that two pairs of NO adsorbate states (bands at 1748–1754 and 1722–1730 cm^{-1} and at 2182–2178 and 2162 cm^{-1}) emerged from the NO adsorbate state as a result of thermal processing. And since the two bands in each pair grew and decreased together, this suggests that they are two distinct, but related surface species. The relative intensities of the bands at 1748–1754 and 1722–1730 cm^{-1} and at 2182–2178 and 2162 cm^{-1} at 200 and 300 °C, respectively, and the precursor state at 1671 cm^{-1} suggests that at these temperatures most NO adsorbate species have migrated to the new sites (responsible for the bands at 1748–1754 and 1722–1730 cm^{-1} and at 2182–2178 and 2162 cm^{-1}). However, the formation of the thermally stable surface nitrosyl complexes depends on the value of the activation barrier. Therefore, this situation depicted in Fig. 2i and j is complex since before the formation of thermally stable surface goldnitrosyl complexes, NO molecules are in a metastable state with respect to both product state/s as well as precursor state. Note that at 200 °C the two bands at 1754–1748 and 1730–1722 cm^{-1} are more intense while the other two at 2182–2178 and 2162 cm^{-1} are small (Fig. 2j), whereas at 300 °C the precursor state at 1671 cm^{-1} seems to remain fairly constant in intensity. However, the bands at 1754–1748 and 1730–1722 cm^{-1} slightly decreased in intensity concomitant with an increase in intensity of the bands at 2182–2178 and 2162 cm^{-1} (Fig. 3j and k). It is tempting to speculate that NO adsorbates associated with the bands at 1754–1748 and 1730–1722 cm^{-1} act as precursor states for the two NO adsorbate states (bands at 2182–2178 and 2162 cm^{-1}).

Very little attention has been given to the surface chemistry of NO on gold surfaces. Only a few reports assign bands in the region 1900 and 1915 cm^{-1} to NO bonded to ionic Au (i.e. $Au^{III}(NO_{\delta}{}^{+})$ and $Au^{I}(NO_{\delta}{}^{+})$, respectively [15,18]; 1817–1820 cm^{-1} due to $Au^{I}(NO_{\delta}{}^{-})$ [15,18]; 1840 due to $Au^{I}(NO)$, 1880 cm^{-1} due to Au–NO and 1800 cm^{-1} due to $Au–NO_{\delta}{}^{-}$ [40]. For Au–TiO_2, bands were observed at 1747 and 1583 cm^{-1} [21], and at 1767 and 1747 cm^{-1} [22]. We have previously observed a band due to Au–NO species at around 1796–1810 cm^{-1} [20], which developed into $Au(NO)_2$ complexes with time by accommodating a second NO molecule into its coordination sphere.

Since bands associated with species absorbing at 1696 and 1654 cm^{-1} appear at lower wavenumbers than for Au–NO complexes reported to date [15,18,20,35], definite assignment of these bands cannot be made at present. However, bands in this region have been reported for NO on Pd and other metals and tentative assignments can be made based on these previous reports (see Tables 2 and 3) [41–46]. The positions of the bands (1696–1690 and 1654 cm^{-1}, Fig. 2) suggests that the NO adsorbate species associated with these bands are highly back bonded [53] since the occupancy of antibonding states ($2\pi^{*}$) of NO molecule show up as a weakened intramolecular bonds and is experimentally observed as a reduced vibrational frequency [18,35–39,53]. The observation that the band at 1654 cm^{-1} disappeared during NO adsorption suggests that the NO adsorbate species associated with this band are rapidly desorbed or more likely dissociate and/or converted to other product species by analogy to previous interpretation [40,54].

The most stable sites for propene adsorption on Au–TiO_2(1 1 0) system was suggested to be at the Au island edge sites involving both Au and TiO_2(1 1 0) support [55]. These sites were found to be populated first. High activity of Au–TiO_2(1 1 0) for the decomposition of SO_2 was explained by suggesting bonding of SO_2 molecule to edge sites involving both Au and support [56]. This interfacial adsorption sites resulted in significant elongation of S–O bonds with respect to free SO_2 molecule, facilitating its dissociation [56]. If the NO adsorbate with absorption band at 1654 cm^{-1} is assigned to a NO adsorbate adsorbed on an edge sites involving both Au and TiO_2 support (i.e. interfacial adsorption sites), it will then be consistent with these previous interpretations [55,56] and also expands on the speculation in the literature that the catalytic reaction site is located on the perimeter of the gold–oxide interface [57]. Another possibility is that the NO adsorbates (band at 1654 cm^{-1}) might be adsorbed on Au atoms in the vicinity of the oxygen vacancy since the presence of the oxygen vacancy in the oxide surface renders Au–TiO_2 chemically active, facilitating dissociation of adsorbates [56]. It is unlikely that the band at 1654 cm^{-1} is due to the fundamental vibrational frequency of N_2O_3 (with a band at 1652 cm^{-1} [58]), nor at 1696 cm^{-1} is within a $HONO_2$ (with bands at 1680, 1319, 961 and 781 cm^{-1} [59]). The fact that: (i) no bands in the region 1700–1690 cm^{-1} were detected on the same catalyst during desorption under identical conditions following adsorption of NO_2; (ii) the bands at 1696 and 1654 cm^{-1} are intense on exposure of the sample to

Table 3
Observed ν(N–O) stretching modes of mononitrosyl adsorbates on Pd and Au metal catalysts [46]

T (K)	Adsorbate	Frequency (cm^{-1})	Assignment	High temperature reached (K)	Frequency (cm^{-1})	Assignment	Comment
Pd/Al_2O_3 [46,80]							
190	CO	1990	Three-fold bridging	457	1925	Atop and step bound	Precursor state (1990 cm^{-1}) transformed into the product state (1925 cm^{-1}) during heat treatment in vacuum
190	NO	1760	Atop bound	446	1680	Atop and step bound	Precursor state (1760 cm^{-1}) transformed into the product state (1680 cm^{-1}) during heat treatment in vacuum
Pd/TiO_2 [63]							
300	NO	1751	Linearly bound	599	1788	Linearly	Mononitrosyl (1788 cm^{-1}) originate from thermal decomposition of nitrates and/or other nitrogen-oxo species
$Au–TiO_2$ [this study]							
300	NO	1690–1695	Bridging sites	575	1754–1748, 1730–1722	Edge bound	Precursor state (1690–1695 cm^{-1}) transformed into the product state (11754–1748, 1730–1722 cm^{-1} and 2182–2178, 2162 cm^{-1}) during heat treatment in flowing He
					2182–2178, 2162	NO^+?	

NO, suggests no or little of higher N_xO_y oxo species have formed. This is partly supported by the fact that adsorbed N_2O_3 surface species has previously been reported at 1904, 1571 and 1305 cm^{-1} on Au^I/Na zeolites [18]. Point (i) above also suggests that the presence of NO_2 impurities in the feed gas (if any) make no contribution to these bands.

It is apparent that the nature of the adsorption sites containing NO species absorbing at 1654 cm^{-1} are different from those containing NO adsorbates with absorption bands at 1696–1690 cm^{-1} (Fig. 2). By analogy with CO on $Au–TiO_2$ [60] and NO on Pd surfaces [46], the band at 1696–1690 cm^{-1} can be tentatively assigned to bridging NO species since bridge bonded NO adsorbates are multiply coordinated and more strongly adsorbed and the (bridging) sites are expected to be populated first (Fig. 2) [61]. In addition, from symmetry arguments, formation of this state (multiply coordinated NO species) will undoubtedly be enhanced at highly coordinated adsorption sites. The results presented in this study (Figs. 2 and 3) demonstrate that the sites containing NO adsorbates with bands at 1754–1748 and 1730–1722 cm^{-1} and at 2182–2178 and 2162 cm^{-1} could only be significantly populated at high temperatures, i.e. the population of these sites is thermally activated. Unlike previous suggestions [62] where linearly bound NO species on Pd sites (observed at elevated temperatures) was suggested to originate from thermal decomposition of nitrates and/or nitrogen-oxo species, this possibility in our study is ruled out since decomposition of nitrates species on the same catalyst following adsorption of NO_2 did not result in the formation of thermally activated NO species. Therefore, a systematic elimination of all possible surface candidate complexes that are likely to make contribution to NO species absorbing at 1754–1748 and 1730–1722 cm^{-1} and at 2182–2178 and 2162 cm^{-1} leave NO adsorbate with a band at 1696–1690 cm^{-1} as the only likely precursor candidate.

TPD studies of NO desorption from Au^I/NaY revealed two peaks at 372 and 452 K [18]. These were attributed to the desorption of NO from bare zeolite and Au^I ions, respectively. The species desorbed at high temperatures, i.e. 573 K (~300 °C) were identified as N_2 and N_2O, followed by evolution of N_2 and O_2 at 737 K (464 °C) [18]. Further, thermal desorption of NO from TiO_2 gave only one small feature at ~150 °C [62]. However, the spectra depicted in Figs. 2 and 3 show that at higher temperatures (i.e. 300 °C) bands characteristic of NO adsorbates are still detected on the surface, indicating that the NO adsorbates reported in this study are thermally more stable than previously observed for Au-zeolites [18]. Therefore the NO adsorbate at 1696–1690 cm^{-1} during the desorption at elevated temperatures behaves in a manner not previously observed on gold surfaces [18], i.e. before desorption and/or decomposition, it transforms into two thermally stable NO adsorbates (bands at 1754–1748 and 1722–1730 cm^{-1}) (Fig. 2f–i) which further transform into further two NO adsorbates with bands at 2182–2178 and 2162 cm^{-1} at temperatures greater than 100 °C (Fig. 2j and k). This transition signals the mobility of NO adsorbate on the surface, i.e. the species migrate to more stable adsorption sites before desorbing and/or undergoing decomposition [55]. The fact that the NO adsorbates with bands at 1748 and 1722 cm^{-1} and at 2182–2178 and 2162 cm^{-1} are more thermally stable suggests that the bonding characteristics of NO adsorbates on these new sites change entirely. The spectra depicted in Fig. 2k show that at high temperatures, only a broad band with poorly resolved maxima is obtained. However, two distinct maxima are clearly resolved on cooling the sample to room temperature (Fig. 2l). This broad feature suggests that several NO

molecules with slightly different stretching frequencies could be formed on several different adsorption sites and high energy defect sites signalling that at elevated temperatures these large Au particles offer more heterogeneous sites than at room temperature (Fig. 2k and l).

The task of assigning thermally activated NO adsorbate species (with absorption bands at 1748–1754 and 1722–1730 cm^{-1} and at 2182–2178 and 2162 cm^{-1}) that display bands that are red and blue shifted, respectively, relative to gas phase NO (1876 cm^{-1}) and at the same time match experimentally observed thermal stability, is difficult, based on the data reported to date [15,20,40]. The previous detection of bands at 1747 cm^{-1} and at 1767, 1747 cm^{-1} for Au–TiO_2 [21,22] and at 1754 and 1722 cm^{-1} in the reaction of laser-ablated Au atoms and NO with high laser power [63] supports our argument that the bands at 1754–1747 and 1730–1722 cm^{-1} (Fig. 2) are due to NO adsorbates bound to Au sites.

It has previously been shown that a band assigned to CO linearly bound to step sites on small particles for Au–TiO_2 was completely absent on large gold particles of the same catalyst (Au–TiO_2) that has been calcined at high temperature [64,65]. It is well documented that Au catalysts prepared by impregnation typically contain large gold particles, depending on the gold concentration [2]. The fact that: (i) only small fraction of the sites containing NO adsorbates with absorption bands at 1754–1748 and 1730–1722 cm^{-1} on large Au–TiO_2 particles (that we believe are present in the catalyst studied here) were populated at room temperature and the population was significantly increased at elevated temperatures (Fig. 2f–k); and (ii) the detection of a band due to NO adsorbates on small ∼6 nm Au–TiO_2 particles in the same region (1748–1747 cm^{-1}) at room temperature and that heating of the Au–TiO_2 in NO to 673 K and cooled to room temperature resulted in slight spectral change [21] suggest that the sites containing NO adsorbate with an absorption band in the region 1748 cm^{-1} are already present on small Au particles and are populated at room temperature. On this basis [21,22,64,65] and coupled with the fact that: (i) the morphological difference between large and small particles is the number of edge sites, and/or surface atoms which are high in small particles [64,65]; (ii) small gold islands interact very strongly with adsorbate [67] and on edge sites [64,68] and are linearly bound [66]; (iii) edge atoms have a higher intrinsic energy than surface atoms [69], it is suggested that during thermal treatment the adsorbed NO molecules migrate from bridging sites (band at 1690–1696 cm^{-1}) to unstable and/or high energy edge Au sites where NO adsorbates are more strongly bound. This assignment is not unreasonable since edge Au atoms with high intrinsic energy [69], and low coordination number [64], would be expected to readily undergo bonding to an adsorbate [67]. The model of thermally activated NO adsorbates reported in this study is consistent with the previous detection of NO adsorbates in the same region (1750 and 1724 cm^{-1}) following the reaction of laser-ablated Au atoms with NO [63]. Formation of these NO adsorbates was reported to be favoured with the use of high laser power [63].

Taking the results in this study together with the previous detection of the band in the region 1747 cm^{-1} [21,22], it is tempting to suggest that the bands in the region, 1754–1747 and 1730–1722 cm^{-1} are Au particle size-dependent. The bands at 1748 and 1722 cm^{-1} are slightly blue shifted to higher wavenumbers (to 1754 and 1730 cm^{-1}) with increasing temperatures (Fig. 2i and k). This is attributed to the interaction of Au sites (to which these NO adsorbates are bonded) with electronegative oxygen atoms (from the dissociated NO) causing increased electron deficiency in the corresponding Au sites [64].

The other pair of bands in the region 2182–2178 and 2162 cm^{-1} are even more difficult to assign. We note that: (i) the band position is expected to probe the oxidation level of the underlying metallic site/s, with increasing frequency of NO band correlating with increasing oxidation state of the adsorption site; (ii) NO bonded to Au^{n+} ($n = 1$ and 3) ions give rise to ν(N–O) in the region 1900–1915 cm^{-1} [18], 1921–1917 cm^{-1} [64] and were reported to be weakly adsorbed [18]; (iii) gold ions can be reduced to metallic gold during drying and/or during calcination [70]. The pre-treatment history of this sample, the position of the bands (2182–2178 and 2162 cm^{-1}) and the high thermal stability of the NO adsorbate giving rise to these bands (at 2182–2178 and 2162 cm^{-1}) argue against the assignment of these bands to NO adsorbed on Au ions.

The infrared spectrum of adsorbed nitric oxide has been extensively studied. The proposed metal-nitric oxide bonding types together with ν(N–O) vibrational frequency ranges have been summarized by Davydov [34]. According to the proposed bonding classification, the NO vibrational frequency in the region 2100–2400 cm^{-1} is due to purely ionic species (NO^+) [34]. The band in this region has previously been observed at 2175 cm^{-1} [71] and at 2195 cm^{-1} [72] and was assigned to adsorbed NO^+ in (NO^+)(N_2O_4) adduct [72]. In addition, the coadsorption of NO and O_2 on TiO_2 and Mn–TiO_2 produced bands at 2210, 2155 and 2210 cm^{-1} for adsorbed NO^+ species [73]. Therefore, it might be argued that the NO adsorbate adsorbed on gold sites spillover to the TiO_2 sites at high temperatures. However, the band associated with NO^+ nitrosyl species was reported to be easily removed by brief evacuation at room temperature suggesting that it is weakly adsorbed. On the contrary, bands at 2182–2178 and 2162 cm^{-1} increase in intensity with increasing temperature during purging with He gas showing that they are thermally stable and strongly bound. Therefore, the thermal stability of the NO adsorbates with absorption bands at 2182–2178 and 2162 cm^{-1} compared to the weakly adsorbed NO^+ species on TiO_2 [73] makes this possibility unlikely. The assignment of the bands at 2182–2178 and 2162 cm^{-1} is still unclear. Recent theoretical calculations shows that the surface Au atoms become more positively charged as the coordination number decreases and this electron depletion is mainly in s/p

orbitals [74]. The existence of such sites on the catalyst surface and the bonding of NO molecules on such sites during thermal treatment cannot be ruled out. In fact the appearance of these bands (2182–2178 and 2162 cm^{-1}) is consistent with the availability of electron deficient and oxidized sites on the surface [74]. Note the bands in this region show significant tailing on both the high and low wavenumber side of the indicated maxima, showing the complex nature of these species. It is also be noted that these bands (2182–2178 and 2162 cm^{-1}) could not be detected on the same catalyst calcined at a different temperature (spectra not shown).

The observation that almost all the surface nitrate and other nitrogen-oxo species are virtually decomposed at 300 °C (Fig. 2l), whereas the transition between these NO adsorbate species is incomplete is consistent with the suggestion that the high energy input needed to drive the transition cannot arise from disrupting NO and/or other nitrogen-oxo bonds only, but involves the breaking of bonds between surface metal atoms [46]. This suggests that the situation depicted in Fig. 2 cannot be described by a hopping of NO molecules between two adjacent adsorption sites since: (i) that will require lower temperatures to effect a complete transition, as depicted in Fig. 2j; (ii) all NO molecules would revert back to the precursor state following cooling the system to room temperature. Since this is not observed, suggested by the remnant bands at 1748, 1722, 2182–2178 and 2162 cm^{-1} (Fig. 2l) after cooling the system to room temperature, different bonding characteristics of NO adsorbates on these sites are implied. Thermally stable NO molecules has previously been explained in terms of multiple interaction between destabilized surface atoms and NO molecules [46]. To the best of our knowledge, we are not aware of the report indicating the ability of NO molecule to reconstruct gold surfaces. However, it is known that for gold surfaces in electrolyte solutions at sufficiently positive potentials anions adsorb specifically and preferentially on steps and enhance the mobility of gold atoms [75]. This anion enhanced mobility of gold atoms (due to strong gold–anion interactions) forms the basis of electrochemical annealing which has been employed to restore the surface order of gold single crystal surfaces [75] and is rationalized in terms of the weakening and/or breaking of Au–Au bonds in favour of formation of strong Au–anion bond, thus facilitating surface diffusion of gold atoms. It is not unreasonable to assume that the stable "Au=NO" complexes detected here might be formed through an alteration of local atomic structure in order to achieve a more stable surface configuration. Once the stable surface configuration is achieved, it is irreversible. Higher temperatures are needed to effect a complete transition (Fig. 2) and are necessary to break Au–Au bonds and the corresponding energy cost is overbalanced by a newly formed "Au=NO" bonds. The thermal activation (suggested by Fig. 2) is typical of adsorbate induced reconstruction and the common driving force being the higher coordination of an adsorbate with destabilized surface Au atom/s which leads to an overall increase in bonding energy. Hence the higher temperatures needed to drive the transition (Fig. 2) indicate that the associated energy barriers are high. Studies on the Au–TiO_2(1 1 0) model system with the aid of STM images carried out under realistic reaction (temperature and pressure) conditions have been reported [76–79]. Disruption of Au–Au bonds [78] and Au–TiO_2 bonds [76] have been proposed and discussed as possibilities to account for the O_2 pressure/temperature induced morphological changes of Au nano particles. Note that at these temperatures transition of NO adsorbate species may occur simultaneous with NO desorption and/or decomposition. It must also be noted that the detailed nature of this Au particle restructuring under the influence of NO molecules at elevated temperatures as used in this study, is poorly understood.

Since both Au($d^{10}6s^1$) and Pd(d^{10}) have similar closed d shell electron configurations, one might expect that models derived for Pd surfaces might be applicable for Au surfaces. However, comparison of the data in Fig. 2 with that for Pd/Al_2O_3 based on the new bonding mode for CO and NO proposed for Pd surfaces give surprising, but at the same time interesting results (Table 3). It is evident from Table 3 that the bands not reported in our work appear on the opposite side of the spectrum compared to those for Pd/Al_2O_3 [46,80] since thermally activated NO adsorbate species for Au–TiO_2 reported in this study appear in the region blue shifted to high wavenumbers relative to NO adsorbate formed at room temperature (precursor state), whereas for Pd/Al_2O_3 they appear to be red shifted [46] (Table 3). The arguments presented to rationalize the bonding characteristics of thermally stable CO adsorbate on Pd/Al_2O_3 surface [80] are not only consistent, but are augmented by the results depicted in Fig. 2. Though no experimental evidence was presented [46], the recognition that once a highly stable surface "Au=NO" complex is formed through multiple interaction, any destabilization of NO adsorbate would be negated by the greater stabilization achieved by the surface Au atom better explains the remnant bands at 1748 and 1722 cm^{-1} and at 2182–2178 and 2162 cm^{-1} after cooling the system to room temperature. Also included in Table 3, is the results for Pd/TiO_2 in which the detection of NO adsorbate band at elevated temperatures on Pd/TiO_2 at positions blue shifted relative to NO adsorbate formed at room temperature was reported. These results are somehow surprising since the description of the bonding characteristics of these NO adsorbates does not explicitly implicate the effect of the support. These interesting chemistry on Pd and Au surfaces hidden behind thermal processing needs further investigation.

Acknowledgements

This work was supported by the National Research Foundation, THRIP, Sasol Technology (Pty) Ltd. and the University of the Witwatersrand.

References

[1] M. Haruta, T. Kobayashi, H. Sano, N. Yamada, Chem. Lett. (1987) 5.
[2] G.C. Bond, D.T. Thompson, Catal. Rev. Sci. Eng. 41 (1999) 319.
[3] M. Haruta, S. Tsubota, T. Kobayashi, H. Kageyama, M.G. Genet, B. Delmon, J. Catal. 144 (1993) 175.
[4] A.M. Visco, A. Donato, C. Milone, S. Galvagno, React. Kinet. Catal. Lett. 61 (1997) 218.
[5] S. Minico, S. Scire, C. Crisafuli, R. Maggiore, S. Galvagno, Appl. Catal. B 28 (2000) 245.
[6] G.Y. Wang, H.L. Lian, W.X. Zhang, D.Z. Jiang, T.H. Wu, Kinet. Catal. 43 (2002) 433.
[7] A. Ueda, M. Haruta, Gold Bull. 32 (1999) 3.
[8] M.C. Kung, J.H. Lee, A. Chukung, H.H. Kung, Stud. Surf. Sci. Catal., Part A and B 101 (1996) 701.
[9] M.C. Kung, K.A. Bethke, J. Yan, J.-H. Lee, H.H. Kung, Appl. Surf. Sci. 121/122 (1997) 261.
[10] A. Ueda, M. Haruta, Appl. Catal. B 18 (1998) 115.
[11] G.R. Bamwenda, A. Obushi, A. Ogata, J. Oi, S. Kushiyama, H. Yagit, K. Mizino, Stud. Surf. Sci. Catal. 121 (1999) 263.
[12] A. Ueda, T. Ohnishi, M. Haruta, Appl. Catal. B 12 (1997) 81.
[13] N.W. Cant, N.J. Ossipoff, Catal. Today 36 (1997) 125.
[14] T.M. Salama, R. Ohnishi, M. Ichikawa, J. Chem. Soc., Faraday Trans. 92 (1996) 301.
[15] S. Qiu, R. Ohnishi, M. Ichikaa, J. Phys. Chem. 98 (1994) 2719.
[16] M. Haruta, Catal. Surv. Jpn. 1 (1997) 61.
[17] J.R. Mellor, A. Palazov, B.S. Grigorova, J.F. Greyling, K. Reddy, M.P. Letsoalo, J.H. Marsh, Catal. Today 72 (2002) 145.
[18] T.M. Salama, T. Shido, R. Ohnishi, M. Ichikawa, J. Chem. Soc., Chem. Commun. (1994) 2749.
[19] S. Qiu, R. Ohnishi, M. Ichikawa, J. Chem. Soc., Chem. Commun. (1992) 1425.
[20] M.A. Debeila, M.S. Scurrell, N.J. Coville, G.R. Hearne, Catal. Today 72 (2002) 79.
[21] F. Solymosi, T. Bansagi, T.S. Zakar, Catal. Lett. 87 (2003) 7.
[22] F. Solymosi, T. Bansagi, T.S. Zakar, Catal. Phys. Chem. Chem. Phys. 5 (2003) 4724.
[23] Y. Li, W.K. Hall, J. Catal. 129 (1991) 202.
[24] M.A. Debeila, M.S. Scurrell, N.J. Coville, G.R. Hearne, J. Phys. Chem. Chem. Phys., submitted for publication.
[25] K. Nakamoto, Infrared and Raman Spectroscopy of Inorganic and Coordination Compounds, Wiley, New York, 1978, p. 1984.
[26] S.-J. Huang, A.B. Walters, M.A. Vannice, J. Catal. 192 (2000) 29.
[27] K. Hadjiivanov, Catal. Lett. 68 (2000) 157.
[28] M.C.P.M. da Cunha, M. Weber, F.C. Nart, J. Electroanal. Chem. 414 (1996) 163.
[29] G. Ramis, G. Bucsa, V. Lorenzelli, P. Forzatti, Appl. Catal. B 64 (1990) 243.
[30] M.M. Kancheva, V.Ph. Bushev, K.I. Hadjiivanov, J. Chem. Soc., Faraday Trans. 88 (1992) 3087.
[31] M.A. Debeila, M.S. Scurrell, N.J. Coville, G.R. Hearne, in preparation.
[32] M.A. Hitchman, G.L. Rowbottom, Coordin. Chem. Rev. 42 (1982) 55.
[33] J.E. Huheey, E.A. Keiter, R.L. Keiter, Inorganic Chemistry: Principles of Structure and Reactivity, 4th ed., Harper Collins College Publishers, New York, 1993, p. 351.
[34] A.A. Davydov, in: C.H. Rochester (Ed.), IR Spectroscopy of Adsorbed Species on the Surface of Transition Metal Oxides, Wiley, New York, 1994 (in preparation).
[35] M.J.D. Low, R.T. Yang, J. Catal. 34 (1974) 347.
[36] L. Cerruti, E. Modone, E. Guglielminotti, E. Borello, J. Chem. Soc., Faraday Trans. 1 70 (1974) 729.
[37] A. Martinez-Arias, J. Soria, J.C. Conesa, X.L. Seoane, A. Arcoya, R. Cataluna, J. Chem. Soc., Faraday Trans. 91 (1995) 1679.
[38] A. Sanis, I. Panas, Surf. Sci. 42 (413) (1998) 477.
[39] J. Laane, J.R. Ohlen, Prog. Inorg. Chem. 27 (1980) 465.
[40] T.M. Salama, R. Ohnishi, T. Shido, M. Ichikawa, J. Catal. 162 (1996) 169.
[41] C. Panja, B.E. Koel, J. Phys. Chem. A 104 (2000) 2486.
[42] G. Pirug, H.P. Bonzel, H. Ibach, J. Chem. Phys. 71 (1979) 593.
[43] T. Lizuka, J.H. Lunsford, J. Mol. Catal. 8 (1980) 391.
[44] M. Bertolo, K. Jacobi, Surf. Sci. 226 (1990) 207.
[45] T.E. Hoost, K. Otto, K.A. Laframborse, J. Catal. 155 (1995) 303.
[46] M.R. Albert, J. Catal. 195 (2000) 62.
[47] G.W. Smith, E.A. Carter, J. Phys. Chem. 95 (1991) 2327.
[48] M.E. Bartram, B.E. Koel, E.A. Carter, Surf. Sci. 219 (1989) 467.
[49] J.Y. Lee, J. Schwank, J. Catal. 102 (1986) 207.
[50] J. France, P. Hollins, J. Electr. Spectrosc. Relat. Phenom. 64/65 (1993) 251.
[51] P. Dumas, R.G. Tobin, P.L. Richards, Surf. Sci. 171 (1986) 579.
[52] F. Boccuzzi, S. Tsobuta, M. Haruta, J. Electr. Spectrosc. Relat. Phenom. 64/65 (1993) 241.
[53] C.M. Grill, R.D. Conzalez, J. Phys. Chem. 84 (1980) 878.
[54] J. Rasco, F. Solymosi, J. Chem. Soc., Faraday Trans. 1 76 (1980) 2383.
[55] H.M. Ajo, V.A. Bondzie, C.T. Campell, Catal. Lett. 78 (2002) 359.
[56] J.A. Rodriquez, G. Liu, T. Jirsak, J. Hrbek, Z. Chang, J. Dvorak, A. Maiti, J. Am. Chem. Soc. 124 (2002) 5254.
[57] M. Haruta, Catal. Today 36 (1997) 153.
[58] C.H. Bibart, G.E. Ewing, J. Chem. Phys. 61 (1974) 1293.
[59] T.G. Koch, N.S. Holmes, T.B. Roddis, J.R. Sodeau, J. Chem. Soc., Faraday Trans. 92 (1996) 4787.
[60] F. Boccuzzi, A. Chiorino, M. Manzoli, D. Andreeva, T. Tabakova, J. Catal. 188 (1999) 176.
[61] H. Conrad, G. Ertl, J. Kuppers, E.E. Latta, Surf. Sci. 65 (1977) 235.
[62] J.M. Watson, U.S. Ozkan, J. Catal. 210 (2002) 295.
[63] A. Citra, X. Wang, L. Andrews, J. Phys. Chem. A 106 (2002) 3287.
[64] F. Boccuzzi, A. Chiorino, M. Manzoli, P. Lu, T. Akita, S. Ichikawa, M. Haruta, J. Catal. 202 (2002) 256.
[65] F. Boccuzzi, A. Chiorino, M. Manzoli, Mater. Sci. Eng. C 15 (2001) 215.
[66] M. Ruff, S. Frey, B. Gleich, R.J. Behm, Appl. Phys. A 66 (1998) S513.
[67] V.A. Bondzie, S.C. Parker, C.T. Campbell, Catal. Lett. 63 (1999) 143.
[68] J.-D. Grunwaldt, M. Maciejewski, P. Fabrizioli, A. Baiker, J. Catal. 186 (1999) 458.
[69] L.D. Marks, D.J. Smith, in: M.L. Deviney, J.L. Gland (Eds.), Catalyst Characterization Science: Surface and Solid State Chemistry, ACS Symposium Series 288, Philadelphia, August 1984, p. 29.
[70] B. Schumacher, V. Plzak, M. Kinne, R.J. Behm, Catal. Lett. 89 (2003) 109.
[71] X. Wang, H.-Y. Chen, W.M.H. Sachtler, J. Catal. 197 (2001) 281.
[72] K. Hadjiivanov, H. Knozinger, B. Tsyntsarski, M. Dimitrov, Catal. Lett. 62 (1999) 35.
[73] M. Kantcheva, J. Catal. 204 (2001) 479.
[74] Z.-P. Lu, P. Hu, J. Am. Chem. Soc. 124 (2002) 14770.
[75] D.M. Kolb, Prog. Surf. Sci. 51 (1996) 109.
[76] A. Kolmakov, D.W. Goodman, Catal. Lett. 70 (2000) 93.
[77] X. Lai, T.P.St. Clair, D.W. Goodman, Faraday Discuss. 114 (1999) 279.
[78] A. Miotello, G. De Merchi, G. Mattei, P. Mazzoidi, C. Sada, Phys. Rev. B 63 (2001) 75409.
[79] C.E.J. Mitchell, A. Howard, M. Carney, R.G. Egdell, Surf. Sci. 490 (2001).
[80] M.R. Albert, J. Catal. 189 (2000) 158.